A Comparative Study on Laser Welding and TIG Welding Of Semi-Solid High Pressure Die Cast A356 Aluminium Alloy

G. Govender, L. Ivanchev, D. Hope, H. Burger and G. Kunene

CSIR, P.O. Box 395, Pretoria, 0001, South Africa
sgovender@csir.co.za , livanch@csir.co.za , dhope@csir.co.za , hburger@csir.co.za , gkunene@csir.co.za

Abstract

Aluminium alloys are used extensively in the automotive and aerospace industries. The development semi-solid forming as manufacturing process has offered the opportunity to HPDC cast complex, near net shape, high volume, and high integrity components. The low porosity levels in SSM high pressure die castings (HPDC) improves the weldability of these components. The aim of the current research was to perform a comparative study of laser and TIG welding of SSM HPDC aluminium alloy A356.

SSM slurries were prepared using the CSIR Rheocasting System and plates of 4mm × 80mm × 100mm were HPDC. Plates in as cast (F), T4 and T6 heat treated conditions were butt welded using a Nd:YAG laser and constant current AC TIG welding. The microstructure and micro-vickers hardness (MVH) properties of the welds were investigated. It was found that the laser welding processes yielded a finer dendritic fusion zone and a much smaller heat affected zone (HAZ) compared to the TIG welds. The HAZ for both the laser and TIG welding was composed of mainly remelted eutectic and substructural changes that were picked up from the MVH profiles. The TIG welding process used was not well suited for eutectic alloys because of the lower energy density. This resulted in partial melting of the root, due to the longer period required for melting the eutectic structure. Collapse of the root and incomplete fusion was observed. The laser welding process was found to be more effective in welding A356 aluminium alloys because of the higher energy density of the process.

1 Introduction

Aluminium alloys are increasingly used in the automotive industry to reduce weight and hence, fuel consumption. High pressure die casting (HPDC) is the most widely used manufacturing process because of its high production rate and relatively low cost to produce high volume, thin walled, complex shaped components. HPDC, inherently, produces components with poor integrity. The high porosity levels encountered reduces the weldability of these components. The development of the semi-solid metal (SSM) processing addresses some of the deficiencies of conventional liquid HPDC. Due to the laminar filling characteristics of SSM HPDC, components with low porosity or porosity free castings can be produced while maintaining the high production rate of conventional HPDC. This improves the weldability of SSM formed components.

The most common welding processes for aluminium alloys in industry are mainly arc welding and resistance welding [1, 2]. Laser welding offers a number of advantages over conventional techniques which include; low and localised heat inputs, high welding speeds, small distortions, minimal loss of material and high quality of final finish [1,2,3]. Laser welding of aluminium alloys therefore offers an attractive alternative to conventional welding techniques. Although a significant amount of work has been done on laser welding of aluminium, very limited research has been done on Al-Si casting alloys [1, 4].

This paper will present a comparative study of laser welding & TIG welding of SSM formed A356 aluminium alloy. A comparative analysis of the microstructure and mechanical properties (MVH) of the two welding techniques investigated is presented.

2 Experimental Procedure

Semi-solid slurries of A356 aluminium alloy were prepared using the CSIR rheocasting system [5]. 4mm × 80mm × 100mm plates were HPDC using a modified 50 ton Edgewick HPDC machine. The plates were inspected using X-ray radiography and plates that had passed X-ray radiography were used in welding experiments. TIG and laser welding of the plates were performed in three conditions, F, T4 and T6. For the T4 heat treatment (HT), the samples were solution treated at 540º C for 6 hours, water quenched and naturally aged for 5 days. The T6 HT employed was as follows: solution treated at 540 ºC for 6 hours, water quenched and artificially aged at 160 ºC for 6 hours.

The laser welds were produced using a Rofin Sinar DY044 diode pumped Nd: YAG laser delivered via 400μm fibre optics. A 200 mm FL HighYAG ASK welding head with twin spot capability was used. The focal plane was positioned on the top surface of the material. The plates were first machined to obtain straight edges for welding. The surfaces to be welded were cleaned using a brass wire brush and degreased with acetone before welding. The welding parameters used were: welding speed – 3m/min, drag angle - 15º, twin spot separation – 0.49mm (in line with weld), 50% helium – 50% argon shielding gas (flow rate 10 l/min) and laser power of 4.4 kW.

The TIG welding was performed using a Miller 330ST Aircrafter (constant current AC/DC arc welding power source) welder. The welding parameters employed were: Argon 5 purge gas (flow rate – 7 l/min), Argon 5 shielding gas (low rate – 10 l/min), 90 Amps AC welding current, 360 mm/min welding speed and A356 filler metal. The filler metal rods were prepared from A356 feedstock. A single V weld design was used for all TIG welds.

Metallographic samples of cross-sections of the welds were prepared and etched using 0.5vol% HF. The general weld profile and structure was observed using stereo microscopy. The microstructures were observed using optical microscopy. The hardness profiles were measured using a Future-Tech FM-700 hardness tester. A 300g load was selected for the microhardness testing. This was selected in order to reduce the noise in the hardness profile because of the difference in hardness between the primary grains and the eutectic structure. Chemical analysis of the base metal and weld zone was performed using a Thermo Electron Quantris optical emission spectrometer (OES). The samples for analysis of the weld zone were prepared by deforming a section of the weld in order to create enough surface area for bulk chemical analysis on the OES.

Results and discussion

2.1 LASER and TIG welds

The typical weld profile obtained for the laser and TIG welding trials are shown in figures 1 and 2. It was evident from figure 1 that the fusion zone for the laser welds was composed of a The HAZ for the laser welded sample was also much smaller than that observed in the TIG welds (figure 2 C). There was visual evidence of partial remelting of the eutectic in the HAZ

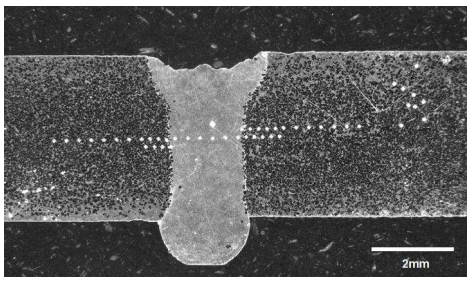

Figure 1: Stereo microscope image of the laser weld profile.

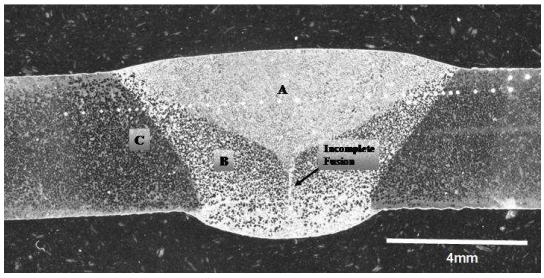

Figure 2: Stereo microscope image of the TIG weld profile.

in the TIG welds (figure 2 B). This resulted in sagging of the root and also contributed to incomplete fusion (figure 2).

The chemical composition of the fusion zone and base metal are shown in table 1. There were no significant differences in composition between the fusion zone and base metal for the laser welds. Since there was no filler metal used in the welding process, the fusion zone was essentially re-melted base metal. The low heat input and short welding time also ensures that there are insignificant losses of volatile elements like Mg and Sr. The only chemical variation of significance that was observed in the TIG weld; was the lower strontium content in the weld zone, due to the vaporisation of the strontium during the welding process.

Table 1 : Chemical Composition of the weld metal of laser and TIG welded A356

	Elements									
	Al	**Si**	**Mg**	**Fe**	**Ti**	**Cu**	**Mn**	**Cr**	**Ni**	**Sr**
Base metal	Bal.	7.23	0.38	0.16	0.107	≤0.005	≤0.005	≤0.005	≤0.005	0.039
Weld metal (laser weld)	Bal.	7.19	0.36	0.15	0.105	≤0.01	≤0.005	≤0.005	≤0.005	0.025
Weld metal (TIG weld)	Bal.	7.49	0.35	0.17	0.13	0.01	0.01	0.007	0.017	0.007

2.2 Micro-Vickers Hardness Profiles

MVH profiles of the laser welds performed on the A356 plates for different pre-weld heat treatment conditions are presented in figure 2. The MVH for the fusion zone of the F, T4 HT and T6 HT after laser welding were very similar (figure 2 and table 2). Solidification of liquid metal occurs in this zone; hence all heat treatment effects are eliminated. The average hardness of the fusion zone of F sample was approximately 21% higher than that of the base metal. This was due to the fine grain structure of the fusion zone. The HAZ of the F sample was relatively small due to the low energy input and short welding time. Since there was no pre-weld HT the energy input into the weld only had localised impact on the hardness at the fusion/HAZ interface.

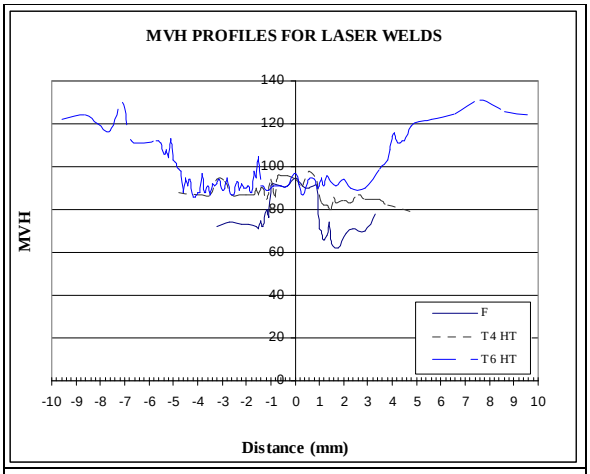

Figure 3 : Micro-Vickers Hardness Profiles of Laser welded samples

Table 2: Average hardness values for base metal and fusion zone after laser welding

	Heat treatment condition		
	As Cast	**T4**	**T6**
Base Metal	72.2	88.7	122.6
Fusion Zone	91.7	91.6	91.2

The T6 HT plates showed a significant drop in hardness in the fusion zone and HAZ due to the re-melting of the fusion zone and the over aging of HAZ. There was no significant difference in hardness between the fusion and HAZ. The T4 heat treated samples showed very little change in hardness between the fusion zone, HAZ and base metal. There was no distinct HAZ zone observable from the hardness profiles since the heat input during the welding process was relatively low and the welding speed high. This minimised the aging effects in the HAZ which equalises its microhardness with that of underaged T4 heat treated base metal.

The MVH profile for the TIG welded samples are shown in figure 4. It should be noted that these profiles only cover the fusion zone and part of the HAZ. A complete profile of T6 HT sample is presented in figure 4b. This shows that the HAZ zone was greater than 30mm. A summary of the MVH values of the base metal and fusion zone for the TIG welded samples are shown in table 3. It was evident that the hardness of the fusion zone was very similar for the welds applied to the plates that had undergone pre-weld heat treatments and the as cast sample. The average hardness of the base metal was consistent with that expected for the heat treatments that were applied and were very similar to the laser welded plates. The average hardness of the fusion zone was found to be approximately 21% lower than that observed in the laser welded samples. The HAZ of the F sample displayed a similar hardness to that of the base metal. The T4 HT samples showed a slight decrease in hardness at the FZ/HAZ interface followed by an increase in the region marked A in figure 4a. The HAZ of T6 HT sample showed an increase in hardness in a narrow zone, approximately 1mm wide. This region had reached the solution treatment temperature for the alloy and had experienced a localised solution treatment. Subsequent mounting of the sample for metallographic examination probably resulted in some artificial aging which accounts for the higher hardness. The hardness of this region was found to be very similar the T4 HT base metal, hence indicating that aging effects due to the sample mounting process was insignificant.

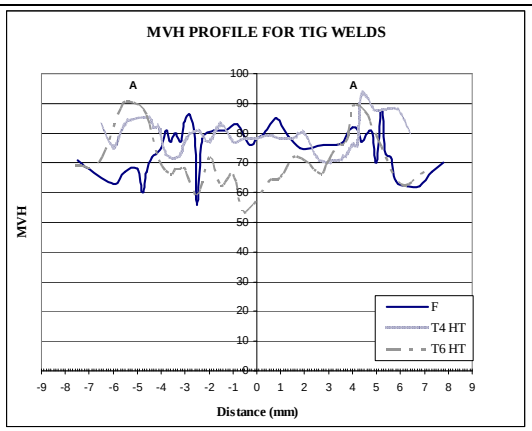

a

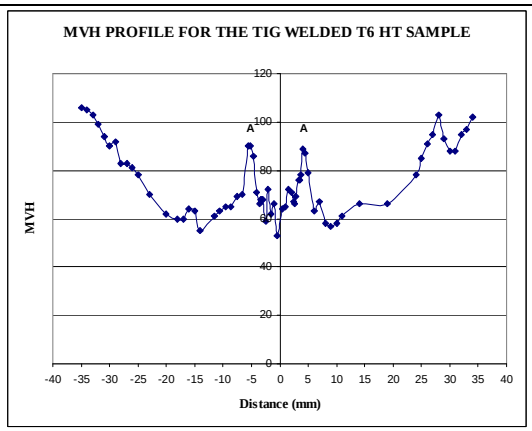

b

Figure 4: Hardness profile for the TIG welded A356 after SSM forming

Table 3: Average hardness values for base metal and fusion zone after TIG welding

	Heat treatment condition		
	F	**T4**	**T6**
Base Metal	68.2	88.2	124.3
Fusion Zone	74.4	72.4	69.8

2.3 Microstructural Analyses

The base metal microstructure of the as cast plate (figure 5) was composed of globular primary α & a fine eutectic structure composed primarily of Al and Si. The base metal microstructures of the T4 HT, and T6 HT samples were found to be very similar (figure 5), consisting of primary globular α and fine spheroidal Si particles. Spheroidisation of the eutectic Si had occurred during the solution heat treatment process. Subsequent aging heat treatment did not show any difference in the final microstructure, however, it was evident from MVH that there were substantial changes in the substructure of the T6 HT plates. This could be as a result of the precipitation of GP-zones,θ", θ' or θ.

The fusion zone for all laser welded samples was composed of a fine dendritic structure (figure 6a). The average secondary dendrite arm spacing (SDAS) was 4.05 μm. This accounts for the higher hardness observed for the fusion when compared with as fabricated sample. The TIG welds displayed a slightly coarser dendritic structure (figure 6b) with an average SDAS of 10.97 μm. This accounts for the higher hardness observed in the fusion zone of the laser welded samples. Although the dendritic structure of the TIG welded plates were coarser than that of the laser welds it does account for the higher hardness values when compared to the as fabricated base metal.

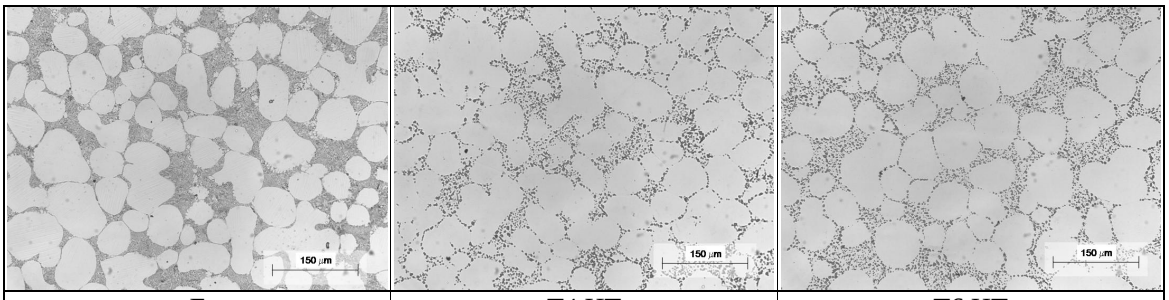

F	T4 HT	T6 HT

Figure 5 : Microstructures of the SSM formed A356 plates

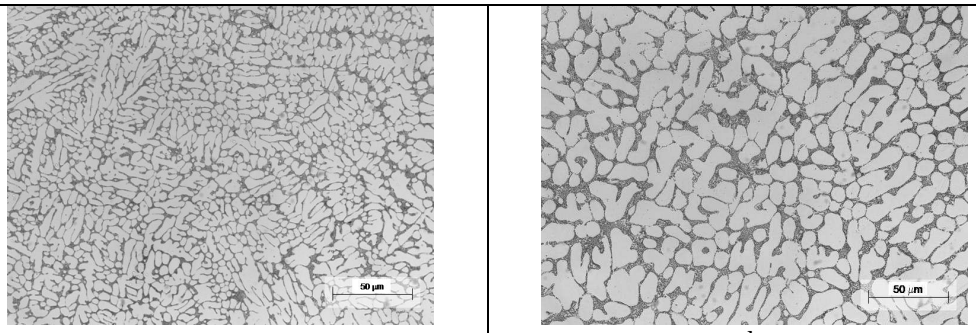

a	b

Figure 6: Typical micrographs of the fusion zone of (a) Laser and (b) TIG welded A256

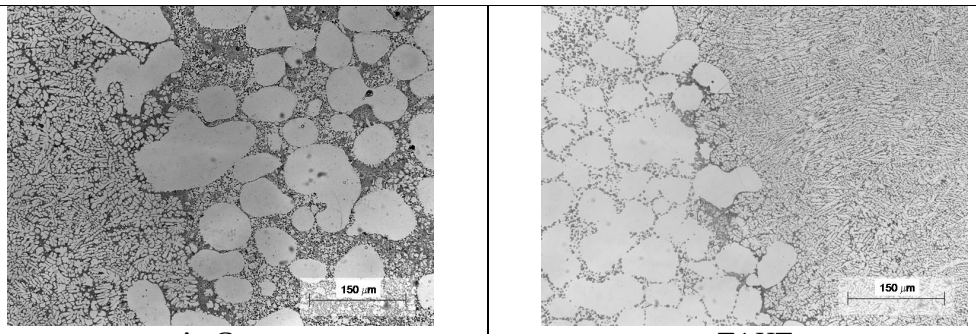

As Cast	T4 HT

Figure 7: Micrograph of the HAZ of laser welded A356

The HAZ for the laser welded as cast and heat treated plates showed minimal structural changes. Figure 7 shows the typical HAZ for the as fabricated and T4 HT plates. The main structural change observed was localised remelting of the eutectic structure immediately adjacent to the fusion zone (figure 7). The microstructural analyses of the HAZ zone shows no visible structural changes, however, it was evident from the MVH profile of T6 preweld heat treated sample that substructural changes do occur.

The HAZ of all the TIG welded samples (figure 8) was composed of remelted eutectic and partial remelting of the α primary grains close to the fusion zone. The remelted eutectic zone was much larger than that observed for the laser welds. The microstructure of region B (figure 2) in the TIG welded samples shows that this region was in the semi-solid condition during the welding process. It was also evident that a significant amount of energy was used in the melting of the eutectic structure which resulted in incomplete melting of the root of the weld. This resulted in incomplete fusion in a number of samples. The semi-solid material at the root of the weld collapsed or began to flow. This indicated that when welding the Al-Si alloys it

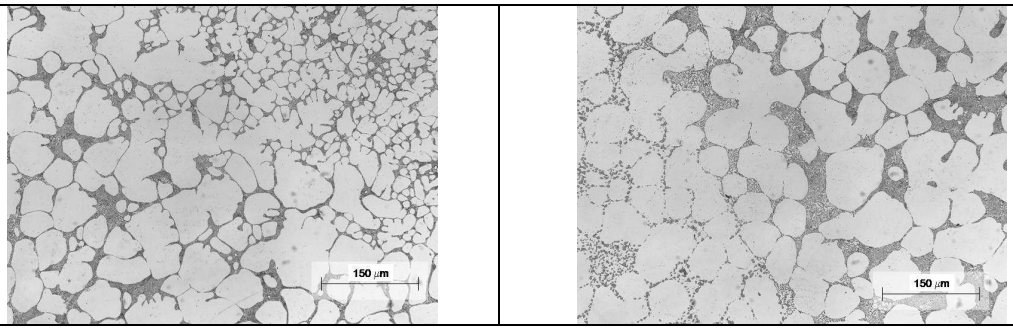

Figure 8: Microstructures of the HAZ of TIG welded SSM formed A356 aluminium alloy (T4 HT)

may be necessary to support the root of the weld. The laser welding process reduces this effect because of the concentrated energy input and rapid welding process. The volume of semi-solid structure formed was relatively small; hence reducing the effects observed in the TIG welds. It was evident that the welding parameters for the TIG welds need to be optimised in order to improve the quality and integrity of welds before a full mechanical property evaluation can be completed.

3 Conclusion

The fusion zone for both the laser welded and TIG welded aluminium A356 consisted of dendritic α primary grains and interdendritic eutectic. The SDAS of the TIG welded samples were approximately 63% greater than the laser welded samples, accounting for the difference in hardness of the fusion zone.

The HAZ of the laser welded samples was much smaller than that of the TIG welded material due to the high welding speeds and lower energy used to complete the weld. The microstructural changes observed were similar for the different HT conditions. It was evident from the T6 HT sample that although there were no visible structural changes, the laser welding process had resulted in substructural changes over a much wider area.

The HAZ adjacent to the fusion zone for the TIG welded samples was composed of remelted eutectic and partially melted primaryα. The energy source for the TIG welding process is less concentrated resulting in heating of a “large” volume of material in the root of weld to the semi-solid state. This contributed to the partial collapse of this zone and incomplete fusion. This phenomenon was not observed in the laser welds because of the higher intensity/more focused energy source. It was evident that the TIG welding parameters used were not suitable for welding of SSM cast A356. Although there was evidence of porosity in the laser welded sample, it was more conducive to the welding of A356.

4 References

1. A. Haboudou, P. Peyre, A.B. Vannes and G. Peix, Mater. Sc. and Eng. A, 363, 2003, pp 40-52.
2. A. Ancona, T. Sibillano, L. Tricarico, R. Spina, P.M. Lugara, G. Basile and S. Schiavone, J. of Mater. Proc. Tech., 164-165, 2005, pp 971-977.
3. M. S. Popa, C. Rus, D. Preja and R. Moldovan, Proceeding of SPIE, Vol. 5776, Bellingham, WA, 2005, pp 68-73.
4. R. Aktar, L. Ivanchev and H.P. Burger, Mater. Sc. and Eng. A, 447, 2007, 192-196.
5. L. Ivanchev, D. Wilkins and G. Govender, Proceedings of the 8th International Conference on Semi-Solid Processing of Alloys and Composites, 21-23 September 2004, Limassol, Cyprus.